

REMOTE SENSING OF VOLCANO-LACUSTRINE INTERACTIONS: IMPLICATIONS FOR MARS. R. N. Greenberger¹, J. F. Mustard¹, E. A. Cloutis², P. Mann², J. H. Wilson³, K. M. Cannon¹, ¹Dept. of Geological Sciences, Brown University, Providence, RI, 02912, Rebecca_Greenberger@brown.edu, ²Dept. of Geography, University of Winnipeg, Winnipeg, MB, R3B 2E9, Canada. ³Headwall Photonics, Inc., Fitchburg, MA, 01420.

Introduction: The conditions of formation for ancient hydrothermal deposits on Mars [e.g., 1-3] have important bearings on the habitability of such systems [e.g., 4-5]. Volcanically resurfaced open basin lakes are abundant on Mars [6], suggesting that past volcano-lacustrine interactions may have occurred. Yet only orbital scale morphologic criteria have been used to assess whether deposits have formed through this process. While excellent work has been done with remote sensing of terrestrial felsic hydrothermal systems [e.g. 7-9], comparable analyses of hydrothermal interactions in mafic systems are more limited. Our goals are to characterize the alteration of lacustrine pillow basalts in the laboratory, measuring changes in mineralogy, chemistry, and spectral signatures with alteration, and scale the measurements to an outcrop to better understand the nature of the water-rock interactions.

Methods: The ~187 Ma Talcott formation basalts [9] erupted within a lake in the Hartford Basin to form hydrothermally altered pillow lavas [e.g., 10-11]. One outcrop in Meriden, CT, was imaged with Channel Systems hyperspectral imagers covering 420-720 and 650-1100 nm, all with 10 nm spectral resolution. Images were calibrated with a dark current subtraction and flat field correction to remove instrument effects and dark object subtraction and correction to in-scene calibration target for atmospheric correction. Spectra of single points were measured from 350 to 2500 nm on the outcrop and on samples with an Analytical Spectral Devices FieldSpec 3 portable spectrometer.

Ten samples from the outcrop were imaged in the laboratory at Headwall Photonics with engineering models of their high efficiency visible-near infrared (VNIR; 400-1000 nm, 1.785 nm spectral resolution) and shortwave infrared (SWIR; 950-2500 nm, 12.0656 nm spectral resolution) hyperspectral imagers. These images are dark-subtracted, ratioed to Spectralon[®], and corrected for the reflectance properties of Spectralon[®]. Spectral variations in mineralogy and oxidation state were mapped by calculating spectral parameters (formulas are given in figure captions) [e.g., 12]. Dedicated mineralogy and chemical analyses are ongoing.

Results: Laboratory imaging. Hyperspectral imaging of samples in the laboratory shows changes with increasing alteration. Secondary phases in a cross-section of a pillow basalt including Fe/Mg-clays (chlorite or smectite) in the rind and Ca-rich carbonate in amygdules and material cutting through the pillow

were mapped with SWIR spectral parameters (Fig. 1a). Carbonates in the outer portion of the rind either have Fe²⁺ in their structures or are mixed with a Fe²⁺-bearing phase. The interior, carbonates, and rind also have different VNIR spectral properties. Interior spectra have a weak positive (red) slope at wavelengths less than 750 nm. The carbonates are almost featureless at these wavelengths but are the brightest phase and are well-mapped by a parameter that is the reflectance at 700 nm. The material cutting through the pillow has a stronger red slope and is brighter overall, consistent with SWIR parameters and spectra indicating a mixture of basalt and carbonate. The alteration rind, visibly green, is mapped by the green peak parameter.

Spectra of the interior of this pillow are consistent with minimally altered basalt (Fig. 1b). A transect across the rind in Fig. 1 shows that a peak in reflectance at green wavelengths becomes more pronounced toward the exterior due to the strengthening of a Fe²⁺/Fe³⁺ charge transfer absorption at 750-800 nm [14-17]. Additionally, a Fe/Mg-OH combination band from a clay mineral appears near 2310 nm [18] and deepens and becomes more asymmetric toward the exterior of the rind. From the spectra, we conclude that the basaltic or glassy matrix was partially oxidized and altered to a Fe/Mg-clay with increasing interaction with water. Other samples toward the base of the section (not shown) have redder rinds that may be mixtures of Fe-oxides and clays and/or carbonates.

Outcrop imaging. Imaging of the outcrop shows similar results. The base of the section (not shown) is dominated by red alteration consistent with what has been interpreted in ocean floor pillow basalts to be initial products of alteration [19]. Higher in the section, the alteration is greener, similar to the rind on the cross-section of the pillow imaged in the laboratory. Based on work by [19], we interpret the greener section of the outcrop to be more altered. Mapping of this unit (Fig. 2) distinguishes interiors and exteriors of pillows and also identifies locations where carbonates or other minerals (e.g., prehnite) have precipitated. These interpretations agree well with ASD spectra and laboratory imaging of samples collected from within images.

Implications: Pillow basalts that were hydrothermally altered in a lacustrine setting show characteristic changes with increasing interaction with water that can be mapped in samples and across outcrops. We therefore predict that degrees of interaction with water can

be inferred from orbital or rover-scale hyperspectral imaging measurements. Alteration rinds can be quantitative indicators of interaction with water [e.g., 20], and we will further investigate these samples to determine if changes in mineralogy and oxidation state determined by spectroscopy also quantitatively relate to the water-rock ratios and conditions of alteration. Qualitatively, red alteration rinds of Fe-oxides and carbonates and/or clays with minimally-altered basaltic interiors dominate the least altered samples. Thicker green rinds of Fe/Mg-clays seem to result from higher degrees of alteration, with the strength of hydration features and metal-OH combination bands in the spectra increasing with interaction with water.

References: [1] Ehlmann B. L. et al. (2011) *Nature*, 479, 53-60. [2] Marzo G. A. et al. (2010), *Icarus*, 208, 667-683. [3] Skok J. R. et al. (2010) *Nature Geosci.*, 3, 838-851. [4] Hoehler T. M.

(2007), *Astrobiol.*, 7, 824-838. [5] Mustard J. F. et al. (2013), *Mars 2020 SDT Report*. [6] Goudge T. A. et al. (2012) *Icarus*, 219, 211-229. [7] Swayze G. A. et al. (2003), *JGR*, 108, 5105. [8] Clark et al. (2003), *JGR*, 108, 5131. [9] Thomas M. and Walter M. R. (2002), *Astrobiol.*, 2, 335-351. [10] Seidemann D. E. et al. (1984) *GSA Bull.*, 95, 594-598. [11] Puffer J. H. et al. (1981) *GSA Bull.*, 92, 515-553. [12] Philpotts A. R. et al. (1996) *J. of Petrology*, 4, 811-836. [13] Pelkey S. M. (2007) *JGR*, 112, E08S14. [14] Burns R. G. (1993), *Cambridge Univ. Press*, 2nd ed., 578 pp. [15] Cloutis E. A. et al. (2011), *Icarus*, 212, 180-209. [16] Cloutis E. A. et al. (2011), *Icarus*, 216, 309-346. [17] King T. V. V. and Clark R. N. (1989), *JGR*, 94, 13997-14008. [18] Clark R. N. et al. (1990), *JGR*, 95, 12653-12680. [19] Alt J. C. et al. (1986), *JGR*, 91, 10309-10335. [20] Hausrath E. M. et al. (2008), *Geology*, 36, 67-70.

Acknowledgments: We would like to thank Dr. Anthony Philpotts for showing us potential field sites in Connecticut and Tim Goudge and Dr. Sandra Wiseman for assistance in the field. We would also like to thank Jeffrey Krug and the staff at Target in Meriden, CT, for allowing us to work on their property and the city of Meriden for permitting us to sample.

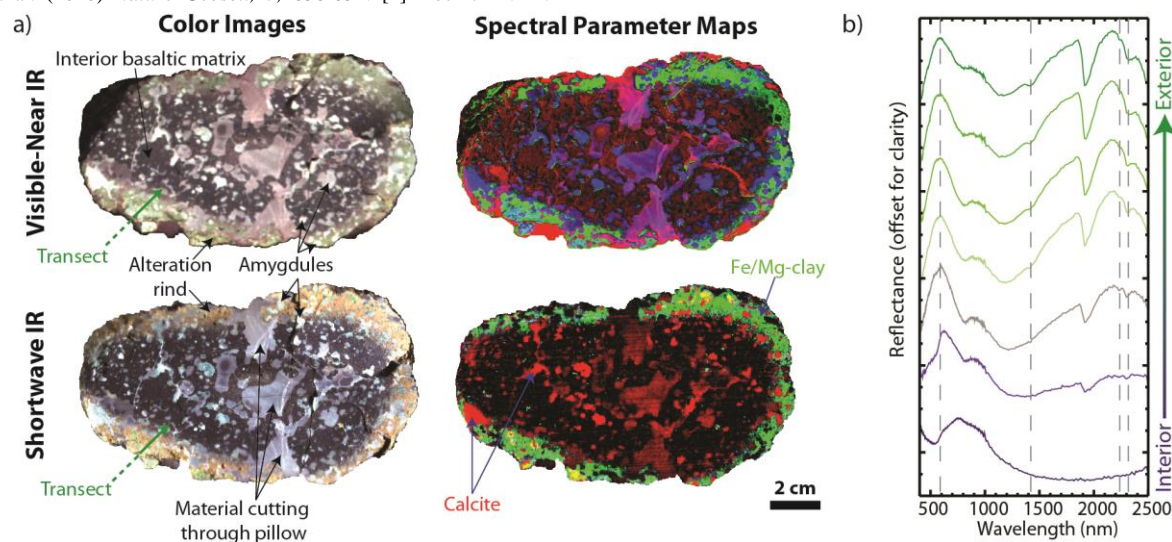


Fig. 1: a) Laboratory images and spectral parameter maps of a cross-section of a hydrothermally-altered pillow basalt. Top left: almost true color image of sample (R: 662, G: 531, B: 426 nm). Top right: VNIR spectral parameter map (R: red slope, G: green peak, B: reflectance at 700 nm). Bottom left: SWIR false-color image (R: 2301, G: 1577, B: 1070 nm). Bottom right: SWIR spectral parameter and mineral map (R: Ca-rich carbonate, G: positive slope due to Fe, B: Fe/Mg-rich clay). Spectral parameters were calculated as follows (Refl = reflectance at some wavelength): red slope = $\Sigma(\text{Refl } 758 \text{ to } 769 \text{ nm}) / \Sigma(\text{Refl } 483 \text{ to } 494 \text{ nm})$; green peak = $2 * \Sigma(\text{Refl } 592 \text{ to } 603 \text{ nm}) / \Sigma(\text{Refl } 465 \text{ to } 476 \text{ and } 747 \text{ to } 758 \text{ nm})$; positive SWIR slope = $\Sigma(\text{Refl } 1790 \text{ to } 1820 \text{ nm}) / \Sigma(\text{Refl } 1150 \text{ to } 1180 \text{ nm})$; Ca-rich carbonate where there are features at 2340 and 2500 nm; and Fe/Mg-rich clay where there is a positive SWIR slope, a feature at 1390 or 1410 nm, a feature at 2300 nm, and a roll-off toward 2500 nm of less than 0.1. b) Spectra from transect across alteration rind. VNIR and SWIR spectra were joined at 998 nm. Position of transect shown in left images in a.

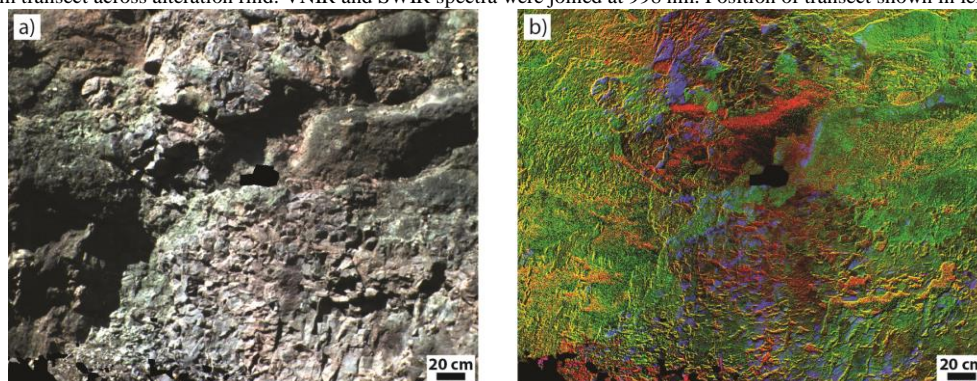


Fig. 2: Imaging of outcrop of hydrothermally-altered lacustrine pillow lavas in Meriden, CT. Vegetation and calibration targets have been masked. a) Almost true color image (R: 660, G: 530, B: 450 nm). b) Spectral parameter map (R: red slope, G: green peak, B: reflectance at 700 nm). Red slope = $\Sigma(\text{Refl } 690, 700, 710 \text{ nm}) / \Sigma(\text{Refl } 440 \text{ to } 450 \text{ nm})$ and green peak = $\Sigma(575 \text{ to } 590 \text{ nm}) / \Sigma(465, 470, 695, \text{ and } 700 \text{ nm})$.